Vibrational states of a H monolayer on the Pt(111) surface

Ş. C. Bădescu,[1] K. Jacobi,[2] Y. Wang,[2] K. Bedürftig,[2] G. Ertl,[2] P. Salo,[3] T. Ala-Nissila,[3,4] and S. C. Ying[4]
[1]*Naval Research Laboratory, 4555 Overlook Avenue, SW, Washington, DC 20375, USA*
[2]*Fritz-Haber-Institut der Max-Planck-Gesellschaft, Faradayweg 4-6, D-14195 Berlin, Germany*
[3]*Laboratory of Physics, Helsinki University of Technology, P.O. Box 1100, FIN-02015 HUT, Espoo, Finland*
[4]*Department of Physics, Brown University, Providence, Rhode Island 02912-1843, USA*
(Received 19 May 2003; revised manuscript received 14 July 2003; published 3 November 2003;
publisher error corrected 6 November 2003)

We present high-resolution electron energy-loss data and theoretical modeling for the vibrational properties of an atomic monolayer of H (D) on the Pt(111) surface. Experimentally we find three loss peaks, in contrast with two peaks visible in the low-coverage case. A three-dimensional adiabatic potential-energy surface at full coverage of hydrogen is obtained through first-principles calculations. When the zero-point energy effects are included, the minimum energy adsorption site is found to be the fcc site just as in the low-coverage case. Vibrational band states for motion in this potential-energy surface are computed and the excited states associated with the observed loss peaks identified.

DOI: 10.1103/PhysRevB.68.205401 PACS number(s): 68.43.Pq, 68.43.Bc, 68.49.Jk, 71.15.Mb

I. INTRODUCTION

The investigation of hydrogen on solid surfaces in general contributes largely to our understanding of adsorption, diffusion, and vibration on surfaces. In particular, Pt surface is one of the most important materials for heterogenous catalysis of hydrogenation reactions. Recently, we have presented a combined experimental and theoretical study for H (D) on Pt(111) at low coverages ($\theta \leqslant 0.75$).[1] In that work we showed that in order to understand the experimental vibrational spectra [measured with high-resolution electron energy-loss spectroscopy (HREELS)], one needs to consider the protonic band structure[2,3] based on the *three-dimensional* (3D) adiabatic potential-energy surface (APES), as derived from first-principles (FP) calculations. Here we extend that study to the case of a full monolayer (ML) coverage ($\theta = 1$). We observe an HREELS vibrational spectrum which strongly deviates from the low coverage case. We propose a qualitative interpretation of the new loss peaks on the basis of FP calculations for the 3D APES for H adsorption at $\theta = 1$.

II. EXPERIMENT

Our experiments were performed in an ultrahigh vacuum apparatus with a base pressure of 3×10^{-11} mbar, consisting of two chambers connected by a valve. The upper chamber is equipped with an argon ion sputtering gun, a low-energy electron-diffraction (LEED) optics, and a quadrupole mass spectrometer used to perform thermal-desorption spectroscopy (TDS) experiments with a heating rate of 5 K/s. The lower chamber housed a HREEL spectrometer (Delta 0.5 SPECS, Germany). The sample was mounted between W wires in narrow slits at its edges and a NiCr/Ni thermocouple was spot welded to the back of the Pt crystal. The temperature could be varied from 85 to 1300 K by combining cooling with liquid nitrogen and heating by radiation or combined radiation plus electron bombardment from the back side. The sample was cleaned by sputtering-annealing cycles as described elsewhere.[4] The chemical cleanliness was checked by HREELS. Gas purities were 99.999% for H_2 and 99.7% for D_2. The H (D) coverage $\theta_{H(D)}$ is given with respect to the number of substrate surface atoms and the exposure is given in units of Langmuir ($1\ \mathrm{L} = 1.33 \times 10^{-6}$ mbar$\times$s).

A series of TD spectra as a function of H_2 exposure at 85 K is reproduced in Fig. 1. At small exposures only one desorption peak (denoted by β_2) is observed, which shifts toward lower temperatures with increasing exposures and which is attributed to the associative desorption of the H atoms. After saturation of the β_2 state a further feature (denoted by β_1) evolves at the low-temperature side. Both peaks have been observed by Christmann *et al.*,[5] and the formation of the β_1 state is interpreted in terms of repulsive lateral interactions between adorbate particles. Calibrating our TDS data with those from the literature obtained with nuclear microanalysis,[6] which is the only method to quantitatively determine hydrogen coverage, we estimated the saturation coverage in our case to be 1.00 ± 0.05 ML. The absolute coverage of H as a function of H_2 exposure is shown in the inset of Fig. 1. At saturation, the amount of the β_2-H is estimated to be 75% of the monolayer.

The HREEL spectra recorded for various H_2 exposures at 85 K are presented in Fig. 2. As reported in Ref. 1, at low coverages ($\theta \leqslant 0.75$ ML) two peaks at 31 and 68 meV are observed, corresponding to the β_2 state in the TD spectra (Fig. 1). After increasing the coverage over 0.75 ML two

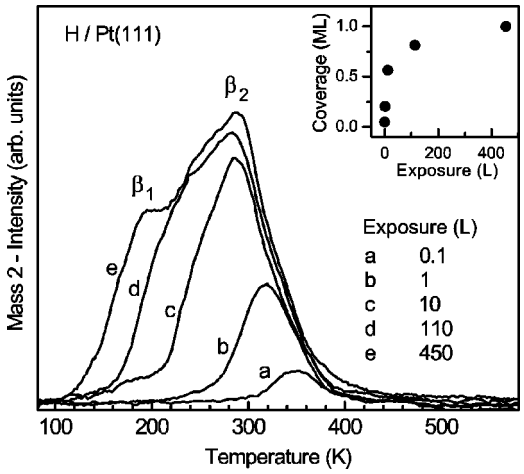

FIG. 1. TD spectra of H_2 (mass 2) for various H_2 exposures in units of L on Pt(111) at 85 K. The heating rate was 5 K/s.

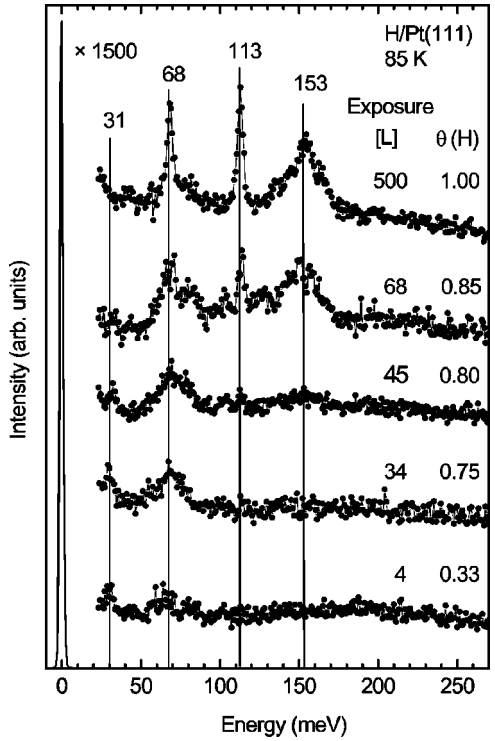

FIG. 2. HREEL spectra of H for different H_2 exposures on Pt(111) at 85 K. Spectra were taken at 85 K in specular geometry with an incidence angle of 55 and with a primary energy of 2 meV.

new losses at 113 and 153 meV appear rather abruptly, simultaneously the peak at 31 meV disappears and the loss at 68 meV gains strongly in intensity. Furthermore, at 1 ML the full width at half maximum (FWHM) of the loss at 68 meV is found to be 4 meV, which is smaller than that ($\approx$20 meV) at low coverages, indicating that this peak is quite different from the one at low coverage. In order to identify unambiguously the H-related losses, isotope substitution measurements with D_2 were performed. The HREEL spectra for H and D at $\theta=1$ ML are shown in Fig. 3. Three peaks at 50, 84, and 111 meV are observed for D. The isotope shifts of 1.35–1.38 clearly confirm the peaks as being due to the vibrational excitations of hydrogen. In summary, at high coverage ($\theta>0.75$ ML) we observe a new spectrum with three loss peaks, suggesting a qualitative change in the state of the H layer.

Up to now there is only one study of the vibrational spectra of the H/Pt(111) system at full coverage by Richter and Ho,[7] and our observed losses agree quite well in energy positions with theirs. The main difference concerns the nature of the peaks. From the dependence of loss intensity on the off-specular angle as shown in Fig. 4, the excited modes associated with the 113 and 153 meV peaks have a clear dipole character. Also, due to the much better energy resolution as compared to Ref. 7, the loss at 153 meV cannot be assigned to an overtone and/or combination loss of the losses at 68 and 113 meV as it was argued in Ref. 7. The dependence of loss intensity on the off-specular angle is the same as in Fig. 4 for all primary energy E_0 values used. In the simple local harmonic model of the vibrational excitations, the finding of two dipole active modes may lead to the idea

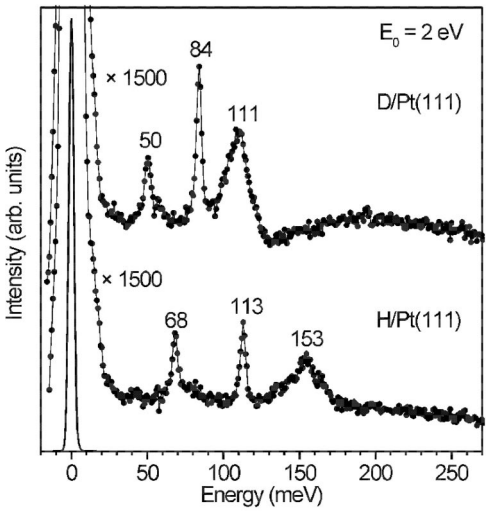

FIG. 3. HREEL spectra for H and D on Pt(111) at $\theta=1$ ML for specular geometry. The primary electron energy is $E_0=2.0$ eV.

that H is adsorbed at two sites on the surface, with different potential curvatures. By speculating further, one can imagine that there is a change in the adsorption site as the H coverage is increased and the APES changes, as it is believed to be the case of H/Ir(111).[8] However, when one goes beyond this simple model and includes anharmonicity as well as delocalization effects as it was done for the low coverage case,[1] the situation is considerably more complicated, and the occurrence of two dipole-character peaks need not imply a change in or simultation adsorption at different symmetry sites. In order to determine the microscopic nature of the vibrational excitations, one has to first evaluate the 3D APES for the full monolayer coverage. Then the vibrational states of the adsorbed hydrogen in this APES need to be determined and compared with the observed excitation loss peaks. We will follow this procedure in this work and compare the results with the simple harmonic picture.

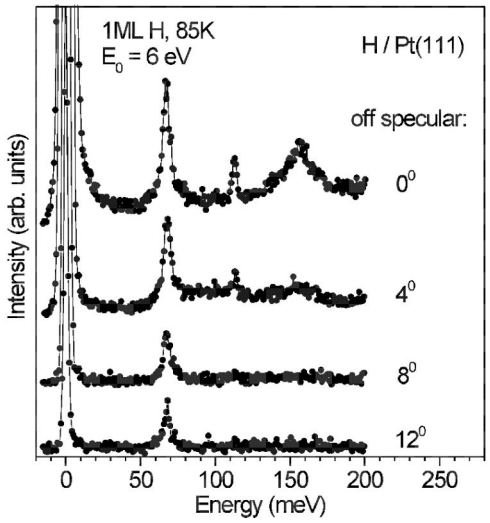

FIG. 4. Comparison of HREEL spectra of $\theta=1$ ML H/Pt(111) for specular and off-specular geometries. The primary electron energy $E_0=6.0$ eV is different from Fig. 4 in order to show the large range of E_0 used.

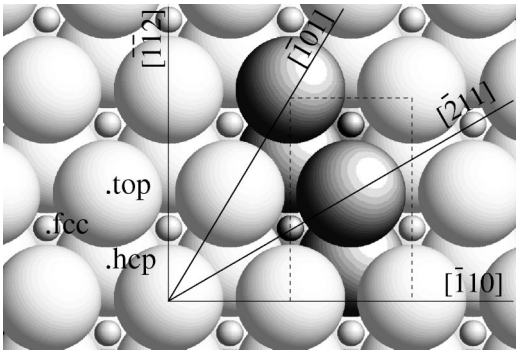

FIG. 5. The Pt(111) slab (large spheres) with one monolayer of H atoms (small spheres) in the fcc position. The atoms in the supercell are represented with darker shading.

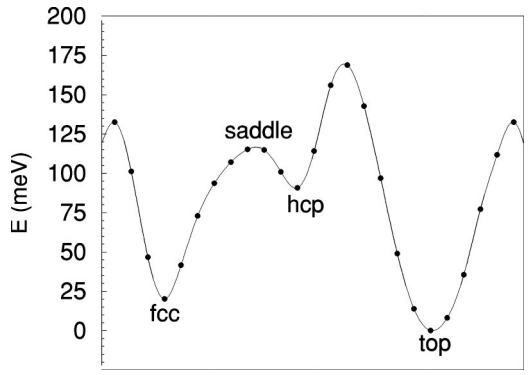

FIG. 6. Minimum-energy path on the APES of H/Pt(111) at 1 ML coverage. The dots are *ab initio* points corresponding to energy minima along the transversal direction; the curve is used to guide the eye.

III. CALCULATIONS

The present APES is calculated with the same self-consistent method as in our earlier low coverage study on the same system,[1] namely a parallel plane-wave code[9] based on density-functional theory with the generalized gradient approximation.[10] We used the Troullier-Martins pseudopotential[11] for Pt and the Vanderbilt nonlocal ultrasoft pseudopotential[12] for H. Electronic wave functions were expanded in a plane-wave basis with a kinetic energy cutoff at 35 Ry, together with a Fermi smearing of 0.2 eV. For the full ML we used a supercell with 8 Pt atoms ($2\times1\times4$) and two H atoms (Fig. 5). We calculated the potential in 65 equidistant planes parallel to the surface, and in each plane at 157 (x,y) positions inside the unit cell of Pt(111). This number insured a smooth interpolation by Fourier transforms (FT's) in plane waves parallel to the surface. In the neighborhood of the on-top site, the values of the potential larger than 6 eV were replaced by gaussians centered at top, connected smoothly with the real APES and with a height of 12 eV, avoiding in this way the divergence of the potential. The H coordinates were also relaxed in the neighborhood of the minima in order to find the minimum energy path (Fig. 6). Only the transversal coordinate of the H atom was relaxed during the calculations, while the Pt atoms were maintained in the frozen structure of the relaxed clean slab. The irreducible Brillouin zone was sampled in this case with 32 $\vec{k}$ vectors.[13] The full APES was built without relaxing the Pt atoms under the action of H, but we studied separately the relaxation of the slab under the influence of H. The distance between the first and the second Pt layers increases by 1.5, 1.9, 1.3%, for H placed at fcc, hcp, and top, respectively. In each of these cases, the variation of the H equilibrium position above the topmost Pt layer changes by -1.1, -0.6, -1.2%, respectively. These geometric variations are in agreement with the experimental data and previous calculations.[14] The relaxation energies are very close in all cases (-29.9, -25.9, -23.2 meV), which suggests an almost uniform shift of the APES by the Pt relaxation due to H adsorption.

In Fig. 6 we show a 1D cut through the APES which demonstrates that the minimum of the potential is at the top site, as opposed to the low coverage case where the fcc site was the absolute minimum.[1] The potential at the fcc and the hcp sites is higher by 22 and 88.5 meV than at the top site, respectively. The barrier between the top site and the fcc site is 131 meV, while that between the fcc and hcp sites is 94 meV. However, these results do not imply that the top site is the lowest energy adsorption site because of quantum effects including zero point energies and delocalization contributions. The zero-point contributions can be estimated using the harmonic approximation based on the local curvatures. In this approximation, the vibrational energy for the parallel motion $\hbar\omega_{\parallel}$ is 77 meV for fcc, and 54 meV for top. For the transversal motion, the corresponding values are $\hbar\omega_{\perp}=142.2$ meV for fcc, and 273.4 meV for top. The latter numbers agree well with the values 147.4–148.4 meV for fcc and 277.0–280.1 meV for top, as calculated by Olsen *et al.*[15] By including the zero-point energies from these harmonic estimates for the vibrational modes, the adsorption energy at the top site becomes now higher than that at the fcc site by 20.6 meV.

To include all the anharmonic effects as well as the delocalization contributions, we diagonalized the effective one-particle Hamiltonian for an H atom using the 3D APES generated in the FP calculations. The vibrational states are expanded in a mixed basis set of plane waves for the parallel directions and localized harmonic oscillator states for the transversal direction. The number of potential FT components obtained above insured a smooth interpolation, and we have chosen the size of the basis set to obtain convergence of the eigenstates.[1] The lowest eigenvalues and eigenstates of the corresponding Hamiltonian matrix are found with the Arnoldi algorithm.[16] The resultant vibrational states form a series of bands with quantum number $(n,\vec{k})$ where n is the band index and $\vec{k}$ the wave vector in the 2D first Brillouin zone. The transition energies are robust against small perturbations of the APES.[1] The low-energy bands are shown in Fig. 7. We also examined the Bloch orbitals for the $\vec{k}=0$ state of each branch. At low energies, these orbitals are mainly confined around the fcc, top, or hcp sites. The overlap between the orbitals centered at adjacent sites is relatively small, leading to a narrow bandwidth. As the energy increases, the states are more delocalized, with orbitals centered at two or three different symmetry sites and having nonzero amplitude in the regions in between, giving rise to wide bands.

The lowest energy band [$n=1$, Figs. 8(a) and (b)] has orbitals localized at the fcc site. The energy of this band is

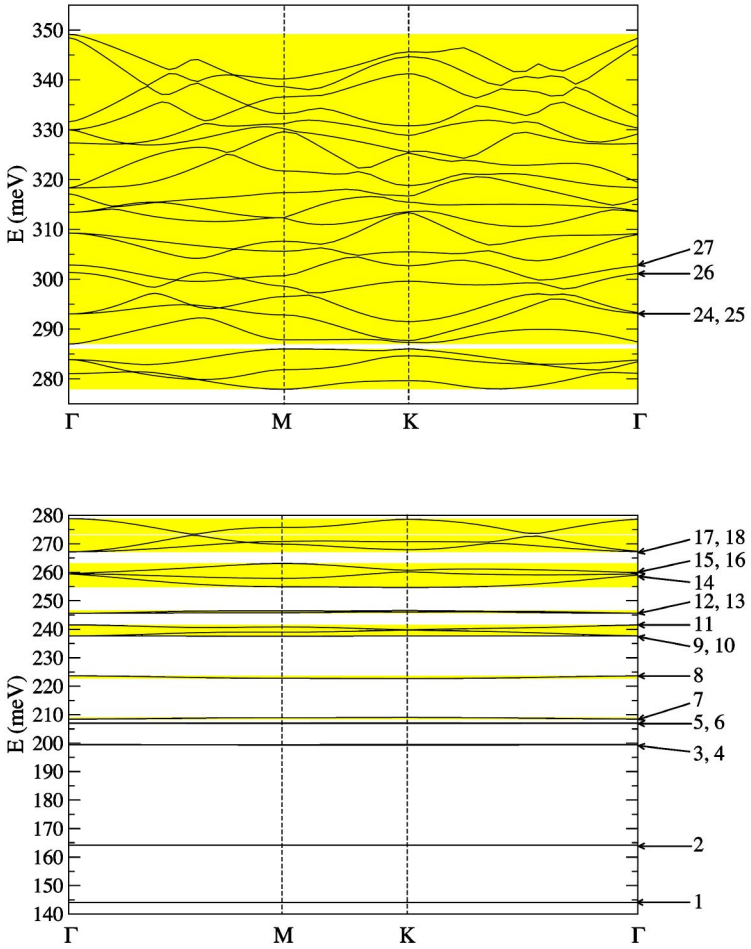

n	localization region	ϵ_n (meV)	$\Delta\epsilon_n$ (meV)
28⊕29	delocalized	308	7.0
		306	5.0
27	delocalized	302	4.0
26	fcc	299	4.0
24⊕25	delocalized	295	6.0
		293	8.0
23	delocalized	289	5.0
n	localization region	ϵ_n (meV)	$\Delta\epsilon_n$ (meV)
17⊕18	hcp	270.4	5.7
		268.8	3.5
15⊕16	fcc-hcp	261.2	5.5
		258.9	2.3
14	fcc	256.2	4.7
12⊕13	top	246.2	0.9
		245.8	0.5
11	top	240.7	1.6
9⊕10	fcc-top	238.7	2.0
		237.6	<0.1
8	fcc	223.1	0.9
7	hcp	208.8	0.5
5⊕6	top	207.0	0.1
		207.0	<0.1
3⊕4	fcc	199.5	0.1
		199.4	<0.1
2	top	164.2	<0.1
1	fcc	144.0	<0.1

FIG. 7. The vibrational branches of H at $\theta=1$ ML. For selected branches, the table shows the degeneracies and the main localization region of the corresponding orbital, the center ϵ_n, and the width $\Delta\epsilon_n$ of each branch.

centered at $\epsilon_1=144$ meV. The next band ($n=2$) has orbitals localized at the top sites with energy centered at $\epsilon_2=164.2$ meV. These values compare well with the estimate of the adsorption site energies including the zero-point energy contributions in the local harmonic approximation. This confirms our earlier assertion that the fcc site remains as the lowest energy adsorption site even though the potential at the top site is lower than that at the fcc site. Both these bands are virtually dispersionless, in accordance with the extreme localized nature of the corresponding orbitals.

At the temperature of 85 K where the HREEL spectra have been measured, the adsorption site is almost exclusively the fcc site. Thus, to interpret the observed loss peaks, we search for excitations from the $n=1$ band state to excited states with orbitals predominantly localized at the fcc site as a candidate for the final state, since this would lead to a larger transition matrix element between the initial and final states. In addition, our mean-field single-particle description for the vibrational bands of the adsorbed H atoms is also more accurate for these relatively more localized states. The first excited band state localized mainly at fcc is double degenerate at $\vec{k}=0$, labeled as $3\oplus4$ [$\vec{k}=0$ orbitals shown in, respectively, Figs. 8(c),(d) and Figs. 8(e),(f)], and originates the asymmetric stretch mode in the local description. The excitation energy from the lowest band $n=1$ to this band is 55.4 meV. We view this excitation as a strong candidate for the first observed loss peak at 68 meV. The energy of the experimental peak is 9 meV lower than the in-plane harmonic frequency estimated from the curvature, and the excitation energy calculated from the vibrational bands is 21.5 meV lower than the harmonic estimation, indicating sizable anharmonic effects. From Fig. 7 one can see that also the states $n=8$ and $n=9\oplus10$ have excitation energies close to the first and second HREELS peak, respectively. However, the $n=8$ state is nondegenerate and has very little lateral and vertical extension, while states $n=9\oplus10$ have most of their weight in the middle between the fcc and hcp sites. Thus we consider these states to be less likely candidates for the HREELS peaks. We also note from Fig. 2 that the experimental loss peak at 68 meV is qualitatively different at high coverages from low coverages. This is in agreement with the fact that the bands currently identified for this transition have a different nature from the wide bands identified at low coverages.[1]

Next, we focus attention on the band $n=26$. The density profiles of the $\vec{k}=0$ orbital for this band shown in Figs. 8(g) and (h) make it clear that it originates from the symmetric stretch vibrational excitation in the local description. The excitation energy of 155 meV to this band state $n=26$ is in good agreement with the location of the third loss peak. The

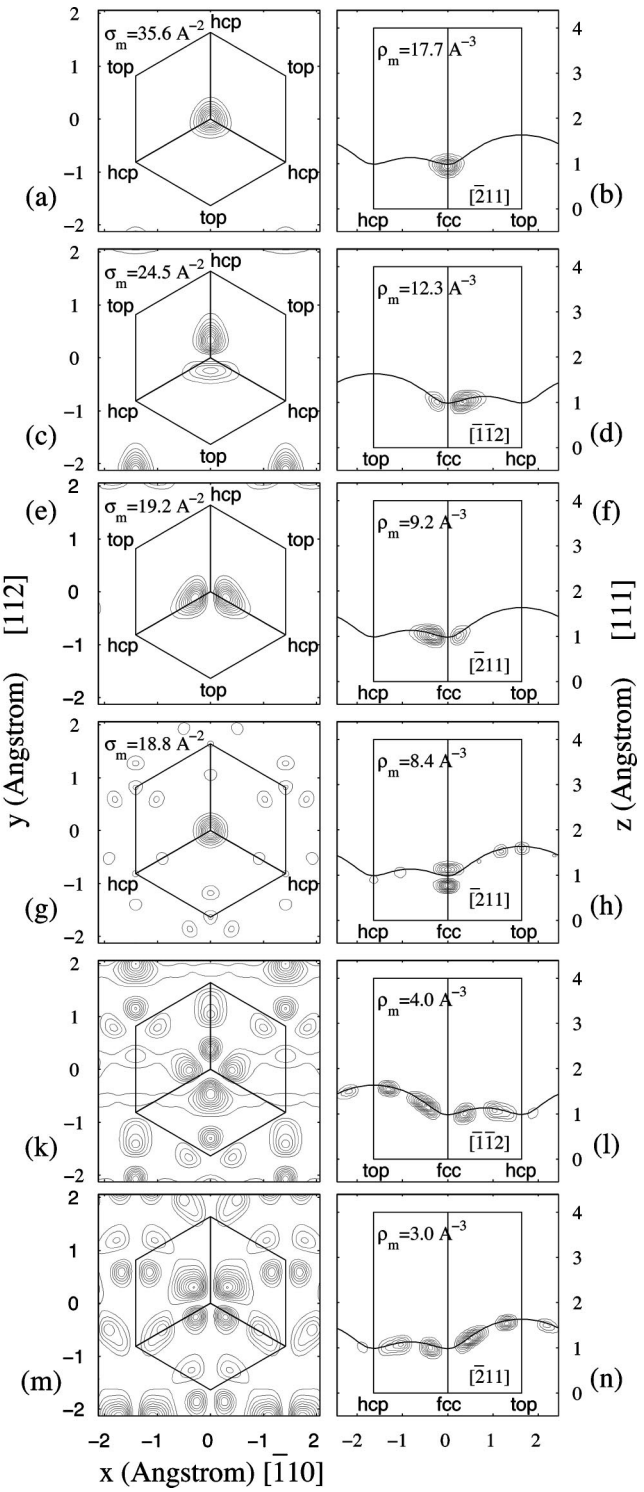

FIG. 8. Orbitals $n=1$ (a,b), $n=3$ (c,d), $n=4$ (e,f), $n=26$ (g,h), $n=15$ (k,l), $n=16$ (m,n). The left column shows the in-plane densities $\sigma(x,y)$. The right column shows probability densities $\rho(\mathbf{r})$ in transversal sections. Ten equidistant contour lines are used in each graph.

energy of this observed mode is very different from the vertical curvature at the on-top site and agrees well with the vertical curvature at the fcc site, supporting the precision of the *ab initio* calculations.

Finally, we discuss the band states $n=14$ and $n=15\oplus 16$, which are all close in energy to the second peak. The orbital for $n=14$ is strongly confined at fcc, while those for $n=15\oplus 16$ have pronounced lobes oriented toward the top sites and raised toward the transversal direction, as shown in Figs. 8(k),(l) and Figs. 8(m),(n), respectively. The excitation energies $\epsilon_{15\oplus 16}-\epsilon_1=115.9$ meV and $\epsilon_{14}-\epsilon_1=112.2$ meV match well with position of the second loss peak. These states cannot be identified with a pure harmonic in-plane mode (asymmetric stretch) or a dipole-active mode (symmetric stretch) at the fcc site. Instead, they are hybrid modes which cannot be described by the simple harmonic oscillator picture. We should note that in the full Hamiltonian including anharmonic and delocalization effects, there is no need to invoke higher harmonics or additional adsorption sites to explain additional loss peaks beyond the simple symmetric and asymmetric stretch modes.

Beyond the low-energy vibrational bands, the higher modes are much more delocalized with larger bandwidth. The matrix elements connecting these states with the lowest localized band are expected to be small. Our mean-field band description may also become unreliable for these bands. Regarding the isotope effect, when H is replaced with D in the previous calculations, we find that the counterparts of the vibrational bands described above with excitation energies from the lowest band are at 42.7 meV (in-plane character, due to states $5\oplus 6$), 91.4 meV (hybrid character, states 14, $15\oplus 16$), and 112.6 meV (dipole-active, due to state 24). These calculated values are in good agreement with the three loss peaks observed for D. The D wave functions are more localized than the H wave functions and the ordering of their energies is different in some cases from that in the H case, as seen for the first and the third transition described above. Nevertheless, the shapes of the states involved in the D spectra have a one-to-one correspondence with the shape of the H wave functions responsible for the H HREEL spectra. In particular, exactly the same considerations as in the H case apply for the wave functions involved in the hybrid mode, which have large weights toward the top site and as such are brought closer to the transversal direction due to the shape of the potential.

IV. DISCUSSION

Our diagonalization method corresponds to a mean-field approximation for the vibrational states of the adsorbed H atoms, where the influence of all other H atoms on the H atom motion under consideration is included only in an average sense. Obviously, this approach cannot account for the full many body nature of the vibrational states. It is expected to be most accurate for those states in which the H wave function is localized near the adsorption sites with relatively small overlaps between adjacent symmetry sites. The first two experimental modes discussed here are in the lower limit of the calculated spectra, while the dipole active mode, even if higher in energy, is very confined in the lateral direction and for that is less affected by the high coverage.

Regarding the vertical transversal excitation found numerically, we mention here that a similar dipole-active mode was found in the low coverage calculation, where the fcc was clearly the adsorption site. In that case the experiments did not identify the peak most likely because of the low transition intensity for that coverage. The position of the experi-

mental dipole-active peak at 153 meV confirms the result of our calculations, namely that the fcc site is the minimum energy site also in the full monolayer coverage. On the other hand, the high value of the potential curvature at top can be viewed in the light of existing calculations for H-Pt hydrides and H-Pt clusters. In the all-electron calculations for the dimers H-Pt, $H\text{-}Pt^{+}$, $H\text{-}Pt^{-}$,[17,18] it was found that the vibrational energy of the hydrogen-platinum bond is between 260 and 277 meV. In Ref. 19, it was found that the H atoms placed on top of Pt atoms in clusters of the type Pt_5-H, Pt_5-H_5, and in the H-Pt molecule, the oscillation frequencies are, respectively, 284.9, 304.8, and 293.2 meV. All HREEL spectra for H/Pt(111) from the literature and the current ones have peaks lower than the values above, which suggest that the H is not in terminal positions. For comparison, a known case of a H/transition-metal system where a site change takes place by increasing the coverage is that of H/Ir(111),[8] where a HREELS peak was observed at 251.7 meV and it was interpreted as a signature of adsorption at the on-top site using the following information: (i) infrared spectroscopy for H_2 adsorbed on an Ir cluster has shown a peak at 254.2 meV;[20] (ii) x-ray structure analysis of $[H_2Ir_4(CO_{10})]^2$ has revealed the formation of terminal H-Ir hydrides;[21] (iii) in infrared adsorption spectra for H adsorbed on Pt electrodes in H_2SO_4 solutions, a band has been observed between 246.7 and 257.9 meV.[22] Despite the remarkable agreement between these experimental values, we know of no FP calculations to confirm the result in Ref. 8.

V. CONCLUSIONS

To conclude, we find that our present theoretical approach can be applied to understand the vibrational excitations of hydrogen on Pt(111) at full monolayer coverage as observed through the loss peaks in HREELS. Our experimental data show three strong vibrational excitation modes, two of them with dipole-active character. The calculations using a full 3D APES show that H (D) adsorbs at the threefold-hollow fcc site when the zero-point energies are taken into consideration. The vibrational data are *not* compatible with the commonly used local harmonic interpretation in which only one dipole-active mode can exist for this site. The key to understand the nature of the observed excitation modes is to recognize that the potential-energy surface is highly anharmonic, leading to strong mixing between the horizontal and dipole-active vibrations of hydrogen as well as additional modes beyond the harmonic picture. We have obtained mean-field single-particle vibrational states of the hydrogen adatom by diagonalizing the Hamiltonian associated with the3D APES. By comparing the character and position of the vibrational excited states with the observed loss peaks, we find that the loss peaks observed at 68 and 153 meV can be identified mainly as the asymmetric stretch (in-plane vibration) and symmetric stretch (dipole-active vibration) at the fcc site, respectively, modified by anharmonic effects. The loss peak at 113 meV, however, cannot be identified with any vibrational mode in the simple localized harmonic oscillator picture. Instead, it is a hybrid mode with both in-plane and dipole character. Furthermore, it has considerable amplitudes at the fcc and hcp sites, and in the region in between these sites. An extended quantum description is necessary for the full understanding of this particular excitation mode.

ACKNOWLEDGMENTS

This work has been supported in part by the Academy of Finland through its Center of Excellence program and by the Galkin Foundation at Brown University. We want to thank Professor T. Rahman for useful discussions. We also wish to thank CSC – Scientific Computing Ltd., Espoo, Finland, for computational resources.

[1] Ş.C. Bădescu, P. Salo, T. Ala-Nissila, S.C. Ying, K. Jacobi, Y. Wang, K. Bedürftig, and G. Ertl, Phys. Rev. Lett. **88**, 136101 (2002).
[2] M.J. Puska, R.M. Nieminen, M. Manninen, B. Chakraborty, S. Holloway, and J.K. Nørskov, Phys. Rev. Lett. **51**, 1081 (1983).
[3] K. Christmann, R.J. Behm, G. Ertl, M.A. Van Hove, and W.H. Weinberg, J. Chem. Phys. **70**, 4168 (1979).
[4] K. Bedürftig, S. Völkening, Y. Wang, J. Wintterlin, K. Jacobi, and G. Ertl, J. Chem. Phys. **111**, 11 147 (1999).
[5] K. Christmann, G. Ertl, and T. Pignet, Surf. Sci. **54**, 365 (1976).
[6] P.R. Norton, J.A. Davies, and T.E. Jackman, Surf. Sci. **121**, 103 (1982).
[7] L.J. Richter and W. Ho, Phys. Rev. B **36**, 9797 (1987).
[8] C.J. Hagedorn, M.J. Weiss, and W.H. Weinberg, Phys. Rev. B **60**, R14 016 (1999).
[9] K. Laasonen, A. Pasquarello, R. Car, C. Lee, and D. Vanderbilt, Phys. Rev. B **47**, 10 142 (1993); S. Pöykkö, M.J. Puska, and R.M. Nieminen, *ibid.* **57**, 12 174 (1998).
[10] J.P. Perdew, K. Burke, and M. Ernzerhof, Phys. Rev. Lett. **77**, 3865 (1996).
[11] N. Troullier and J.L. Martins, Phys. Rev. B **43**, 1993 (1991).
[12] D. Vanderbilt, Phys. Rev. B **41**, 7892 (1990).
[13] D.J. Chadi and M.L. Cohen, Phys. Rev. B **8**, 5747 (1973); S.L. Cunningham, *ibid.* **10**, 4988 (1974).
[14] P.J. Feibelman, Phys. Rev. B **56**, 2175 (1997).
[15] R.A. Olsen, G.J. Kroes, and E.J. Baerends, J. Chem. Phys. **111**, 11 155 (1999).
[16] K. Maschhoff and D. Sorensen, PARPACK code, http://www.caam.rice.edu/~kristyn/parpack_home.html
[17] K.G. Dyall, J. Chem. Phys. **98**, 9678 (1993).
[18] M. Sjøvoll, H. Fagerli, O. Gropen, and J. Almlöf, Int. J. Quantum Chem. **68**, 53 (1998).
[19] X. Xu, D.Y. Wu, and B. Ren, Chem. Phys. Lett. **311**, 193 (1999).
[20] F. Bozon-Verduraz, J. Contour, and G. Pannetier, C.R. Seances Acad. Sci., Ser. C **269**, 1436 (1969).
[21] G. Ciani, M. Manassero, V.G. Albano, F. Canziani, G. Giordano, S. Martinenzo, and P. Chini, J. Organomet. Chem. **150**, C17 (1978); E.L. Muetterties, T. N. Rhodin, E. Band, C.F. Brucker, and W.R. Pretzer, Chem. Rev. (Washington, D.C.) **79**, 91 (1979).
[22] H. Ogasawara and I. Masatoki, Chem. Phys. Lett. **221**, 213 (1994).